

Zeeman splitting of laser-driven soft x-ray laser line by the enhancement of magnetic field in plasma

T Kawachi¹, N Hasegawa¹, A Iwamae² and H Yoneda³

¹Quantum Beam Science Center, Japan Atomic Energy Agency (JAEA),
8-1-7, Umemidai, Kizugawa, Kyoto, 619-0215, Japan

²Faculty of Engineering, Fukui University, 3-9-1 Bunkyo, Fukui, 910-8517, Japan

³Institute of Laser Science, University of Electro-Communications,
1-5-1, Chofu, Tokyo, 182, Japan

E-mail: kawachi.tetsuya@jaea.go.jp

Abstract. We observed a laser-driven plasma soft x-ray laser (SXRL) line at the wavelength of 18.895 nm from the nickel-like molybdenum ions under the existence of external magnetic field. In this experiment, 4 mm-diameter magnetic coil driven by an electrical pulsed power supply provided the external magnetic field of 15 T along the direction of the plasma column, and we could obtain the left-handed circular and right-handed circular polarization components separately. The experimental Zeeman splitting indicated that the strength of the magnetic field was enhanced by a factor of more than 10 than that of the applied field, which implied that the compression of magnetic field occurred in the dynamics of intense laser-plasma interaction.

1. Introduction

Polarized light sources have been widely used as powerful probe in many research fields such as material science, plasma science, biological and medical science and so on. In particular, the circular dichroism measurement has been established in the visible and hard x-ray region, which enables us to obtain the information of the 3-D structure of the materials such as classification of the optical isomer (chirality) [1]. In these wavelength regions transmission optics as phase control devices of the circularly polarized light are available, whereas in the soft x-ray region, effective method to generate and control the circular polarization is not established yet. Recently, the circularly polarized soft x-ray has been generated in synchrotron undulators [3]. However this requires still large facility, and it is difficult to obtain the right-handed and left-handed polarization at the same time.

In this paper we propose an alternative method to obtain circularly polarized intense soft x-ray source using Zeeman splitting of laser-driven plasma soft x-ray lasers (SXRL) [4-6]. We took the transition of the $3d^9 4p$ ($J = 1$) - $3d^9 4d$ ($J = 0$) of the nickel-like molybdenum ions at a wavelength of 18.895 nm as an example, which was well-known as a strong lasing line in SXRL in collisional excitation scheme. We applied the external magnetic field to the gain-medium plasma and investigated the polarization components of the lasing line. This study is valuable as the demonstration of compact intense polarization x-ray source, and at the same time, it is quite interesting in terms of plasma physics, *i.e.*, the influence of the laser-plasma interaction on the magnetic fields in plasma. In the following, the details of the experiment and the analysis are described.



2. Experimental arrangement

Figure 1 shows the simplified experimental arrangement. A thin rod molybdenum target (the cross section was $1\text{ mm} \times 1\text{ mm}$ square and length was 30 mm) was set at the center of the small magnetic coil. Nd:glass laser at a wavelength of 1053 nm was weakly focused on the target surface under the grazing incident pumping (GRIP) configuration [7,8]. The laser light consisted of the pre-pulse and main pulse. The role of the pre-pulse is to generate a pre-formed plasma, by which the following main pulse can be effectively absorbed in plasma to generate population inversion. The total energy on the target was 12 J, and the energy ratio of these pulses was 1 : 4, respectively. The pulse separation was 2.0 ns, and the duration was 400 ps and 7 ps, respectively. The direction of the polarization of Nd:glass laser was perpendicular to the target surface. The grazing incidence angle was $\theta = 14$ degree, and the focal width and length were $60\text{ }\mu\text{m}$ and 5 mm, respectively. The electron density at which the laser light was mainly absorbed was given by $n_{cr} \sin^2\theta = 6 \times 10^{25}\text{ m}^{-3}$, where n_{cr} is the critical electron density at the wavelength of 1053 nm ($= 10^{27}\text{ m}^{-3}$). The magnetic coil, the diameter of 4 mm and 5 mm-length, consisted of winding copper sheet covered by polyimide foil. It is driven by a pulse power supplies with 20kV to obtain the magnetic field of 15 T. The raise up time of the magnetic field is around 800 ns, and the maximum field strength was sustained for several tens ns, which is sufficiently long compared with duration of the XRL pulse. ($< 10\text{ ps}$ [9]).

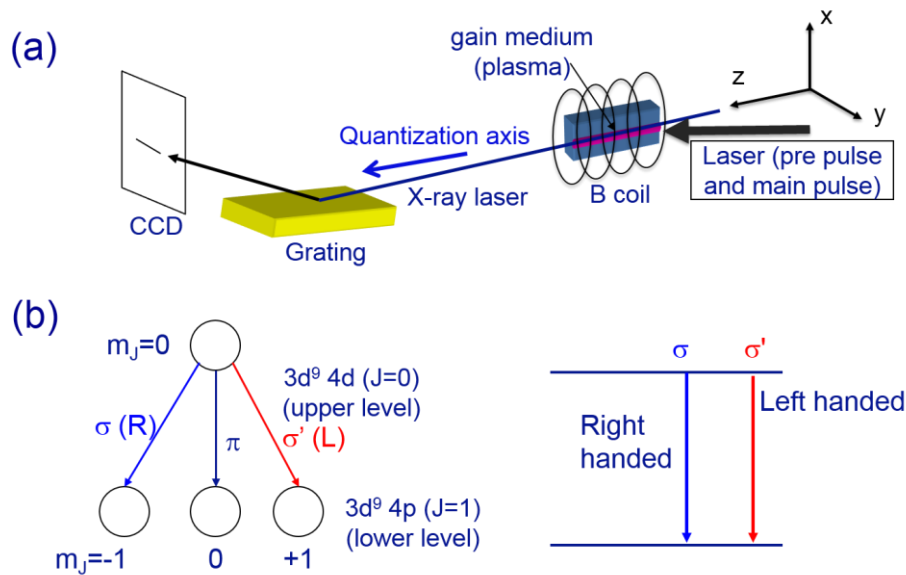


Figure1. Simplified experimental set-up; (a), and Kastler diagram of the lasing line; (b).

In the following context, we define the direction of the magnetic field, *i.e.*, z-axis in Fig. 1, as the quantization axis. Figure 1(b) shows the Kastler diagram of the lasing transition, $3d^9 4d (J=0)$ levels $\rightarrow 3d^9 4p (J=1)$. The lower lasing level ($3d^9 4p$ level) has three magnetic sublevels with $m_J = -1, 0, 1$, and the SXRL has three polarization components, *i.e.*, left-handed circular (σ'), linear (π) and right-handed circular polarization (σ). The SXRL beam is generated in the z-direction, therefore only the σ and σ' components could be observed. Under the sufficient magnetic field, the degeneracy of the lower magnetic sublevels can be resolved by the Zeeman effect, and we can extract the two polarization components separately. The advantage of this method is that the right- and left-handed circularly polarized SXRL are obtained at the same time.

The Zeeman splitting of the SXRL line was observed by a high-resolution spectrograph, HIREFS (Hetttrick scientific) [10]. Figure 2 shows the optical arrangement of this spectrograph. The $3\text{ }\mu\text{m}$ -width entrance slit of the spectrograph was put at a distance of 70 mm from the edge of the

SXRL gain medium plasma, and the image of the SXRL at the slit was relayed to the detector position through a concave grating and two grazing imaging mirrors. The magnification factor in the direction of x -axis in Fig. 1 (a) (= the direction of the plasma expansion) and y -axis (= the direction of the wavelength dispersion) were 2.4 and 3.2, respectively. The inverse linear dispersion of HIREFS was measured to be 0.0785 nm / mm on the focal plane by using the Carbon Balmer α line (18.220 nm) and Ni-like Mo XRL line (18.895 nm). The back-illuminated CCD camera (Princeton, PI-SX:1K, pixel size 13 μ m) was used for the detector, which corresponded to the spectral resolution of 0.00126 nm ($d\lambda/\lambda = 6.7 \times 10^{-5}$) [11]. The spatial resolution of HIREFS in the direction of the wavelength dispersion was 9.6 μ m, therefore the resolution in the wavelength was mainly determined by the CCD pixel size.

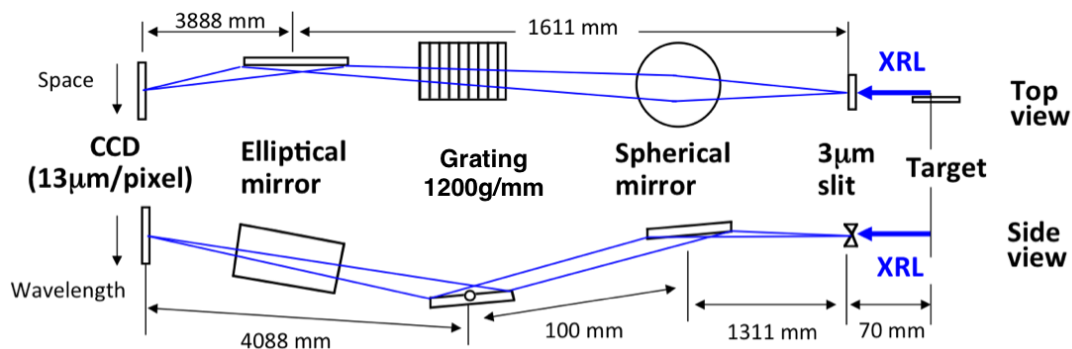


Figure 2. Schematic diagram of the optical arrangement of HIREFS spectrograph.

3. Results and discussion

At first we observed the gain narrowing of the nickel-like molybdenum SXRL line. We changed the plasma length from 3 mm to 5 mm and obtained apparent gain narrowing effect as shown in Fig. 3. The experimental uncertainty for the 3 mm case was larger than that of 5 mm case. This was because the intensity for the 3 mm case was weak due to small amplification effect. The linewidth of the lasing line for the 3 mm plasma length was 36 mÅ. Approximately this linewidth could be treated as the intrinsic linewidth of the lasing line which was the convolution of homogeneous and inhomogeneous broadening. Our theoretical population kinetics model including plasma parameters, *i.e.*, electron temperature and density, implied that the homogeneous and inhomogeneous broadening was 28 mÅ and 15 mÅ, respectively. These values were almost consistent with the total linewidth obtained in the experiment.

Figure 4 (a) shows the spectrum of the lasing line without (upper) and with (lower) the external magnetic field. The vertical and horizontal axes show the wavelength and the refraction angle of the SXRL, respectively. Apparent split was obtained under the presence of the magnetic field, and these two components correspond to the left-handed circular (σ') and right-handed circular polarization (σ). The separation of the two components becomes larger as the refraction angle increases. The SXRL beam is typically refracted due to the density gradient in the gain medium plasma. Since the density gradient becomes steep as the electron density increases, the large refraction angle of the SXRL indicated that the source of the SXRL is in higher density region. That is, the magnetic field strength is higher as the electron density increases. Figure 4 (b) shows the spectral profiles of SXRL line at the position of (A) ~ (E) with the magnetic field in Fig. 4 (a). Under the assumption of linear Zeeman effect, the amount of the split is described as $2\Delta\epsilon = \{J(J+1)\}^{1/2} \mu_B B$ ($= 1.6 \times 10^{-4} B$ [eV]), where μ_B is the Bohr magneton and B is the magnetic field strength. This leads to the magnetic field strength of (A) 40 T, (B) 120 T, (C) 180 T, (D) 220 T, (E) 270 T, respectively; these values are quite high compared with the applied field, and this implies an alternative mechanism to enhance the magnetic field in plasma.

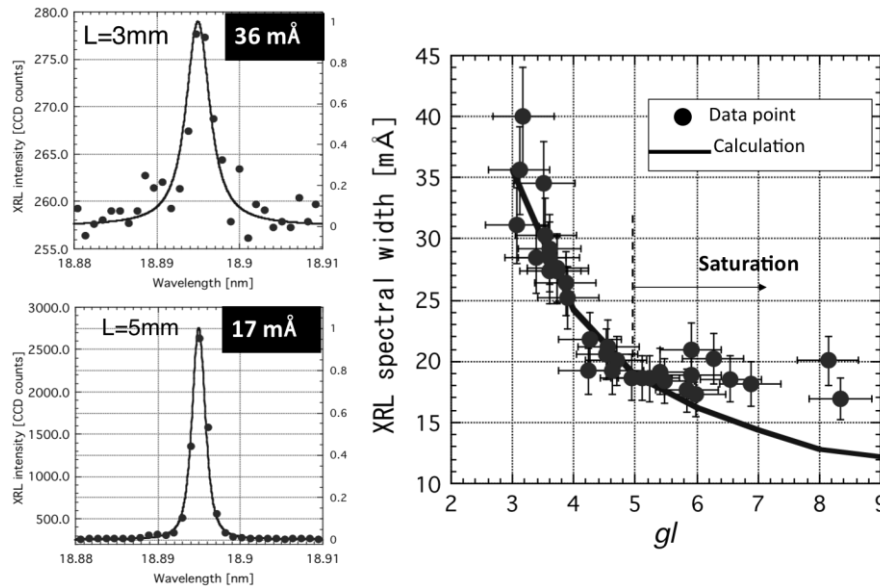


Figure 3. The linewidth of the lasing line with the plasma length of $L=3\text{ mm}$ and $L=5\text{ mm}$. Apparent gain narrowing effect can be seen; (left-hand side). The linewidth of the SXRL line as the function of the gain-length product. For the plasma length longer than 5 mm, we can see the saturation behaviour; (right hand side).

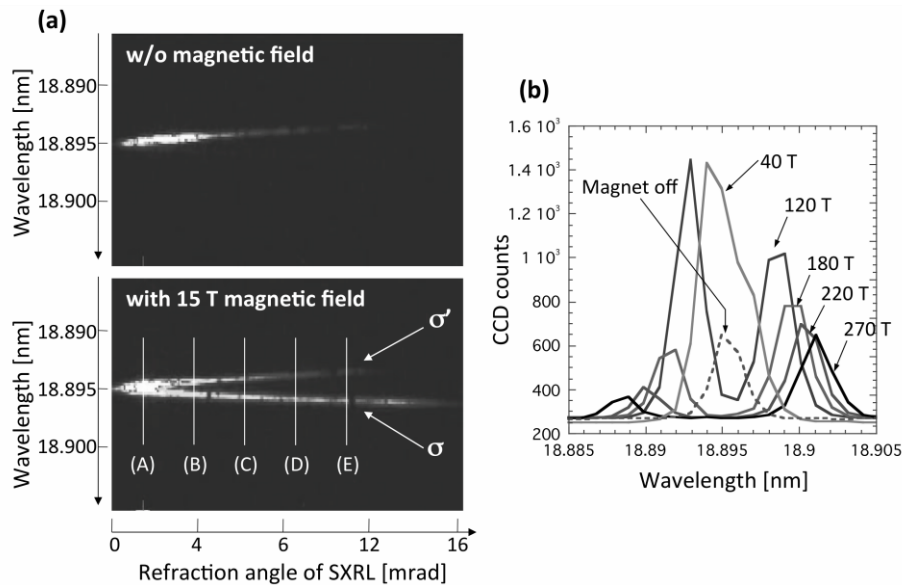


Figure 4. The obtained spectrum of the lasing line without (upper) and with (lower) the external magnetic field. The vertical and horizontal axes show the wavelength and the refraction angle of the SXRL, respectively; (left-hand side). The spectral profiles of SXRL line at (A) ~ (E) in (a). The Zeeman split of these profiles correspond to the magnetic field of (A) 40 T, (B) 120 T, (C) 180 T, (D) 220 T, (E) 270 T. These values are larger by a factor of 8~20 than that of the applied magnetic field.

Enhancement of compression of the magnetic field in laser-produced plasmas has been reported in several previous works, and the compression mechanisms are explained by the shock wave [12] and ponderomotive force [13, 14]. The spatial compression of the magnetic field requires ‘frozen in’

condition in the magnet hydrodynamics (MHD) equation. This means that the change of the electron density distributions due to the compression has to be faster than the relaxation time, t_c , of the magnetic field which is given by $t_c = \mu R^2 / \eta$ [s], where η , μ and R are an resistivity, a magnetic permeability and the size of the gain region, respectively. η is in proportion to the collision frequency and is in proportion to $T_e^{-3/2}$, therefore large t_c can be obtained in high temperature plasmas such as the SXRL gain medium.

Indeed our theoretical investigation using 1D hydrodynamics simulation, HYADES [15] shows that sufficient plasma condition, $T_e = 0.8$ keV, $n_e = 6 \times 10^{25} \text{ m}^{-3}$ and $R \sim 30 \text{ } \mu\text{m}$, can be obtained at the position of the generation of SXRL gain at the time of 5-10 ps after the main laser pulse. From this estimation, the relaxation time of the magnetic field leads to be $t_c \sim 16 \text{ ns}$ ($\eta \sim 7 \times 10^{-8} \text{ Vm/A}$, $R \sim 30 \text{ } \mu\text{m}$). This relaxation time is sufficiently long compared with the gain duration and the time for hydrodynamics motion near the critical density region, that is, and the spatial compression of the magnetic field can occur under sufficiently fast change of the electron density profile in plasma. It is noted that the hydrodynamics simulation indicated that the shock wave is not effective in the present plasma condition, rather, the possibility of the drift of the plasma by ponderomotive force of laser pulse is realistic.

Under the present experimental condition (GRIP scheme), the ponderomotive force (F_p) originated from the gradient of the laser electric field pushes the plasma electrons in the direction of the density gradient (= x -direction), and the plasma is drifted to the higher density region with the lines of the magnetic force. We estimate the amount of the drift as follows: F_p is described as follows:

$$F_p = -\frac{1}{4} n_e \cdot m_e \cdot c_0^2 \nabla \left(\frac{qE}{m_e \omega_{Laser} c_0} \right)^2 \left[\text{N/m}^3 \right] \quad , \quad (1)$$

where, n_e , m_e , c_0 , ω_{Laser} , q and E are electron density, electron mass, light velocity, angular velocity, electric charge and the strength of the electric field, respectively. We assume the electric field of the pump laser is Gaussian profiles, *i.e.*, $E(r, t) = E_0 \exp[-4\ln 2 (r+r_0)^2 / \phi^2] \exp[-4\ln 2 (t-\tau)^2 / \tau^2]$, then F_p can be described as

$$F_p = 5.86 \times 10^{-5} \frac{n_e I_0}{\omega_{Laser}} \frac{r+r_0}{\phi^2} \exp\left(\frac{-4\ln 2 (r+r_0)^2}{\phi^2}\right) \exp\left(\frac{-4\ln 2 (t-\tau)^2}{\tau^2}\right) \quad . \quad (2)$$

Here, ϕ , τ , t , r , and r_0 are the focal spot size of the pump laser, the duration, the time, the distance between the electron position and the laser axis at time t and that of the initial condition, respectively. Under the present laser parameters, $\lambda_{Laser} = 1053 \text{ nm}$, $\phi = 60 \text{ } \mu\text{m}$, $\tau = 7 \text{ ps}$, $I_0 = 4.4 \times 10^{19} \text{ W/m}^2$, the peak of F_p is obtained to be $1.2 \times 10^{14} \text{ N/m}^3$ at $r = 20 \text{ } \mu\text{m}$ and $n_e = 6 \times 10^{25} \text{ m}^{-3}$.

The pressure of the ponderomotive force was estimated from F_p and the thickness of the plasma ($\sim 100 \text{ } \mu\text{m}$), *i.e.*, $1.2 \times 10^{10} \text{ N/m}^3$. It was larger than the internal pressure of plasma ($= 8.2 \times 10^9 \text{ N/m}^2$, at $T_e = 0.8 \text{ keV}$) estimated from the result of HYADES code. The drift length of the electron depends on the initial position of the electrons (r_0) as shown in Fig. 5. Since this calculation does not include the repulsive force due to the compression, the validity of the result is limited to the qualitative estimation. In Fig. 5, for the initial positions of $r_0 = 30.0$ and $40.0 \text{ } \mu\text{m}$ (initial distance = $10.0 \text{ } \mu\text{m}$), the drifted positions are estimated to be 60 and $61 \text{ } \mu\text{m}$ (distance = $1 \text{ } \mu\text{m}$) at the time of $7 \times 10^{-12} \text{ sec}$. Therefore more than 10 times spatial compression of the magnetic field can be expected. Present estimation indicates that the combination of the external magnetic field and the following spatial compression of magnetic field by the intense laser pulse is quite effective to generate higher transient magnetic field

and is applicable for the extraction of the right- and left-handed circularly polarized XRL. For the detailed understanding of this dynamics, further analysis is needed.

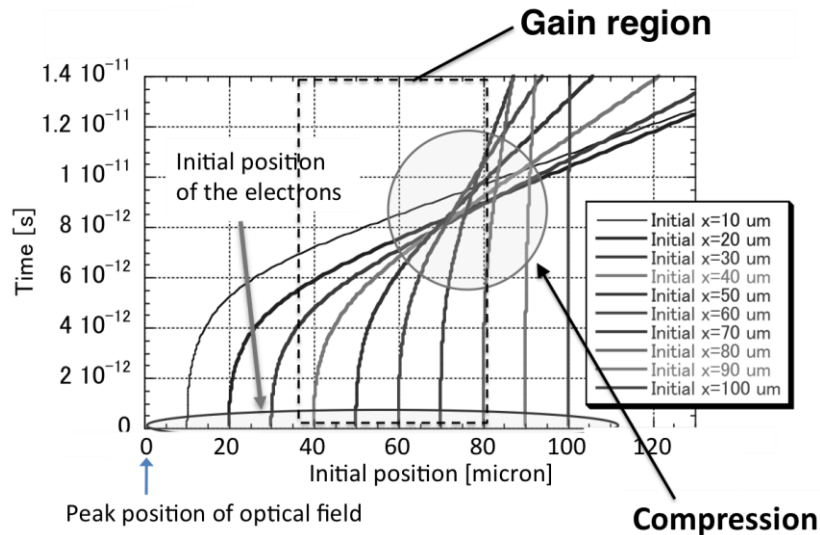


Figure 5. Rough estimation of the drift of the electrons for various initial positions. Due to the pondermotive force, electrons at each position are pushed into the higher density region and plasma compression occurs. For the time $t > 8 \times 10^{-12}$ s, several lines begin to cross each other, and this time region is out of the validity of the calculation. This is because the repulsive force due to the compression is not included in the model calculation.

4. Summary

In summary, we have demonstrated the extraction of right- and left-handed circularly polarized x-ray lasers using the Zeeman splitting. Under the external magnetic field of 15 T together with the spatial compression of the magnetic field by the pondermotive force of the laser pulse, the effective magnetic field is enhanced by around 10 times larger, and we could observe the resolvent of the degeneracy of the magnetic sublevels of the nickel-like molybdenum XRL line at the wavelength of 18.895 nm. Present analysis is limited to the quantitative analysis, and detailed analysis including the coupling of pondermotive force with hydrodynamics motion of the plasma is requires for the deep understanding of this dynamics.

Acknowledgement

This work was partly supported by Grand-in-Aid of Scientific Research (B) (No.25289244) and Grant-in-Aid for Young Scientists (B) (No. 19740350, 22740267) from the Japan Society for the Promotion of Science (JSPS). We thank Professor H. Nishimura, Institute of Laser Engineering (ILE) in Osaka University for his help to use HIREFS spectrometer and thank the x-ray laser crew in JAEA for their support to conduct the experiment.

References

- [1] Fasman G D (Eds.) 1996 *Circular Dichroism and the Conformational Analysis of Biomolecules* (New York: Plenum Press)
- [2] Hirano K, Okitsu K, Momose A and Amemiya Y 2001 *Advances in X-Ray Chemical Analysis, Japan* **33** 25
- [3] Tanaka M, Nakagawa K, Agui A, Fujii K, Yokoya A 2005 *Phys. Scr. T* **115** 873
- [4] Kalachnikov M P, Nickles P V, Schnürer M, Sandner W, Shlyaptsev V N, Danson C, Neely D, Wolfrum E, Zhang J, Behjat A, Demir A, Tallents G J, Warwick P J and Lewis C L S 1998 *Phys. Rev. A* **57** 4778
- [5] Zeitoun Ph, Faivre G, Sebban S, Mocek T, Hallou A, Fajardo M, Aubert D, Balcou Ph, Burgy F, Douillet D, Kazamias S, de Lacheze-Murel G, Lefrou T, le. Pape S, Mercere P, Merdji H, Morlens A S, Rousseau J P and Valentin C 2004 *Nature* **431** 23
- [6] Luther B M, Wang Y, Larotonda M A, Alessi D, Berrill M, Marconi M C, Rocca J J and Shlyaptsev V N 2005 *Opt. Lett.* **30** 165
- [7] Keenan R, Dunn J, Shlyaptsev V N, Smith R F, Patel P K and Price D F 2003 *Proc. SPIE* **5197** 213
- [8] Luther B M, Wang Y, Larotonda M A, Alessi D, Berrill M, Marconi M C, Rocca J J and Shlyaptsev V N 2005 *Opt. Lett.* **30** 165
- [9] Ochi Y, Kawachi T, Hasegawa N, Sasaki A, Nagashima K, Sukegawa K, Kishimoto M, Tanaka M, Nishikino M and Kado M 2004 *Appl. Phys. B* **78** 961
- [10] Hettrick M C, Underwood J H, Batson P J, and Eckart M J 1988 *Appl. Opt.* **27** 200
- [11] Li Y, Nilsen J, Dunn K and Osterheld A L 1998 *Phys. Rev. A* **58** R2667
- [12] Tomasel F G, Shlyaptsev V N, and Rocca J J 1996 *Phys. Rev A* **54** 2474
- [13] Sudan R N 1993 *Phys. Lett.* **70** 3075
- [14] Sandhu A S., Dharmadhikari A K, Rajeev P P, Kumar G R, Sengupta S, Das A, and Kaw P K 2002 *Phys. Lett.* **89** 225002
- [15] Pert G J 1983 *J. Fluid Mech.* **131** 401